Angewandte Chemie International Edition

Angewandte International Edition Chemie

GDCh German Chemical Society

How to cite: *Angew. Chem. Int. Ed.* **2026**, e6835315
doi.org/10.1002/anie.6835315

COMMUNICATION Hot Paper

Conformation-Adaptive Crown Ether-Polyimides as Superfast and Exceptionally Selective Artificial Na^+ Channels

Fei Gou | Yilin Yao | Qiuting Wang | Wenju Chang | Jie Shen | Huaqiang Zeng

Fujian Provincial Key Laboratory of Molecular Synthesis and Functional, Discovery and College of Chemistry, Fuzhou University, Fuzhou, Fujian, China

Correspondence: Huaqiang Zeng (hqzeng@fzu.edu.cn)

Received: 22 March 2026 | **Revised:** 3 April 2026 | **Accepted:** 9 April 2026

Keywords: artificial sodium channels | high selectivity | polyimide | supramolecular chemistry | transmembrane transport

ABSTRACT

The development of artificial Na^+ channels that simultaneously achieve high permeability and high selectivity remains a formidable challenge, as existing systems are constrained by a limited performance ceiling. To address the classical permeability–selectivity trade-off, we present an adaptive design strategy that moves beyond conventional rigid-pore architectures. The system is based on a flexible polyimide backbone functionalized with 15-crown-5 ionophores via tunable alkyl linkers (C_nH_{2n+1}, n = 8–16), enabling efficient Na^+ permeation through multiple adaptive mechanisms. The conformational plasticity of the architecture facilitates dynamic and cooperative ion coordination during capture and transmembrane transport. The best-performing transporter, **4**, exhibits a high Na^+ conductance of 48.9 pS, which is twice that of gramicidin A-mediated K^+ transport, together with a record Na^+/K^+ selectivity of 37.8. This work establishes a new benchmark for synthetic ion transporters and opens promising avenues for the development of biomimetic membranes and therapeutic applications.

Sodium ions function as essential signaling molecules and key electrolytes in biological systems [1–3]. Specialized protein channels, such as the epithelial sodium channel, precisely regulate transmembrane Na^+ flux, a process critical to numerous physiological functions—including nerve impulse propagation, blood pressure regulation, and epithelial fluid secretion [4, 5]. The physiological significance of these channels is further highlighted by channelopathies resulting from their dysfunction, such as Liddle syndrome, pseudohypoaldosteronism, and certain forms of hypertension [6, 7]. Natural sodium channels achieve a unique combination of ultrafast ion conduction (> 10^7 ions/s) and exquisite selectivity (Na^+/K^+ > 500), a benchmark that has inspired yet eluded synthetic chemists for decades [8–10].

The remarkable biological performance has inspired substantial efforts toward developing artificial ion-transport systems, with notable successes achieved across multiple domains [11–47]. Synthetic water channels, for instance, now surpass aquaporin 1 in permeability by 150% while fully excluding salts and protons [48, 49]. Artificial proton channels demonstrate exceptional selectivity, with 167.6-fold preference for H^+ over Cl^-, 122.7-fold over Na^+, and 81.5-fold over K^+, while achieving proton transport rates 1.22 times that of gramicidin A [50]. Similarly, advanced potassium channels have attained K^+/Na^+ selectivity ratio of 153.2 [51] through extensive design and optimization by different groups [23, 31, 33, 35, 42, 47]. And among artificial Li^+ channels [41, 52–54], the highest Li^+/Na^+ and Li^+/K^+ selectivity ratios have also reached 17.7 and 21.8, respectively [54].

In stark contrast, progress in the development of artificial Na^+ channels has been considerably slower and more challenging. In particular, efforts toward precise ion recognition and highly

selective transport remain at an early stage. To date, only a limited number of artificial sodium channels have been successfully constructed and explicitly reported [55–59]. These systems are not only markedly fewer than their potassium channel counterparts, but also display substantially inferior performance. Notably, the best-performing artificial Na^+ channel reported thus far exhibits a maximum Na^+/K^+ selectivity of 13.0 [59]. Although this value demonstrates the feasibility of biomimetic design, its pronounced deviation from the near-perfect discrimination achieved by natural channels represents not merely an incremental limitation, but a fundamental barrier that continues to impede practical application.

Polymers, distinguished by their synthetic versatility and structural tunability, represent an attractive platform for constructing transmembrane channels capable of spanning the ~3 nm hydrophobic core of lipid bilayers [48–54, 60–66]. Among these, polyimides (**PI**s) are particularly attractive owing to their exceptional stability and processability [67–69]. However, conventional aromatic **PI**s generally exhibit poor compatibility with phospholipid bilayers, primarily due to the mismatch between their rigid backbones and the dynamic, flexible lipid environment. We therefore hypothesized that transitioning from rigid frameworks to dynamic, adaptive architectures is essential for achieving effective membrane integration. This design principle is inspired by biological systems, in which efficient ion conduction often relies on soft, conformationally flexible structures that can adapt to the evolving energy landscape of transmembrane permeation [70–74].

Therefore, we engineer a synthetic transporter comprising a conformationally flexible polyimide backbone functionalized with 15-crown-5 ether ionophores through systematically tailored alkyl linkers (C_nH_{2n+1}, n = 8–16). This design harnesses the intrinsic adaptability of the polymeric scaffold combined with the linker-mediated tunable dynamics to facilitate Na^+ permeation via a spectrum of cooperative transport mechanisms. The resulting conformational plasticity enables efficient ion capture and transmembrane transport through dynamically coordinated processes. Among the five synthesized polymeric transporters, four demonstrate notably high Na^+ conductances (29.7–48.9 pS) coupled with Na^+/K^+ selectivity up to 37.8—approximately tripling the previous selectivity record (~13) for artificial sodium channels. This achievement not only establishes a new benchmark in synthetic Na^+ transport system, but also introduces a versatile and dynamic design platform with substantial potential for biomimetic membrane technologies and channelopathy-directed therapeutic development.

Implementation of our "structural adaptability and dynamic function" design strategy starts with the synthesis of a flexible, heteroatom-rich polyimide (**PI**) backbone containing multiple carboxyl groups, obtained via one-pot polycondensation of diethylenetriaminepentaacetic dianhydride and diaminopropane at 180°C (Scheme S1). Gel permeation chromatography (GPC) confirms an average molecular weight of ~7000 Da with approximately 17 carboxylic acid groups per chain, providing abundant functionalization sites while preserving the backbone flexibility essential for structural adaptability.

Subsequent covalent conjugation of 15-crown-5 ether units was accomplished through ester linkages with alkyl spacers of defined lengths (C_nH_{2n+1}, n = 8, 10, 12, 14, 16) (Figure 1a and Scheme S1). Successful grafting is evident from marked differences in solubility: whereas the **PI** polymer dissolves readily (> 50 mg/mL) in $CHCl_3$, DMF, and DMSO, polymers **1**–**5** are nearly insoluble in $CHCl_3$ and DMF and exhibit moderate solubility (> 20 mg/mL) in DMSO (Table S1). NMR characterization also confirms that crown ether groups have been attached to the **PI** polymer backbone (Figures S26–S31). Their molecular weights were determined using GPC, giving rise to 12.0, 13.6, 13.8, 15.8, and 17.9 kDa for polymers **1**–**5**, respectively (Table S2). Additionally, given the strong correlation between the C/O mass ratio (M_C/M_O) in the polymers and the degree of crown ether functionalization (Table S3), we further employed EDS analysis to determine the functionalization degree of polymers **2**–**5** (Figure S1). Compared to the unmodified **PI** polymer (M_C/M_O = 2.12), the M_C/M_O values of polymers **2**–**5** show a gradual increasing trend (Table S4), revealing the crown ether functionalization percents of 30% to 40% for polymers **2**–**5**.

Drawing on relevant literature [20, 27, 38–40, 45–47, 75–78], we believe that the inherent flexibility of the polymer backbone should enable adaptive intercalation into phospholipid membranes, while the crown ether termini spontaneously embed within the hydrophobic core, driven by hydrophobic interactions. We propose that this molecular architecture supports adaptive Na^+ transport through a combination of dynamic processes (Figure 1c), including: (1) a relay mechanism involving coordinated ion transfer between adjacent binding sites [39–40, 46, 75]; (2) a swing mechanism, where individual crown ether units facilitate ion translocation via pendulum-like motions [38, 45, 76–78]; and (3) transient formation of channel-like pathways through convergent assembly of multiple crown ethers [31, 42, 47, 63, 66]. This inherent mechanistic plasticity allows the system to dynamically regulate its transport behavior through multiple complementary pathways, rather than a single mechanism, in response to local membrane conditions and ionic environments, thereby realizing the structural adaptability and dynamic function envisioned in our design strategy.

UV-Vis spectroscopy was used to monitor changes in the interaction between alkali metal ions and the polymers in blank vesicles (without HPTS). Upon the addition of NaCl, the UV absorption spectra of polymers **2**–**5** show pronounced changes, characterized by a decrease in absorbance at 290 nm ranging from 12.3% to 15.0%. By contrast, the addition of K^+ results in a much weaker response (6.7%–9.9% decrease), and Li^+ induces only a negligible change (1.9%–4.9% decrease; Figures S2–S5 and Table S5). These findings demonstrate that **2**–**5** selectively recognize Na^+ ions over K^+ and Li^+.

Binding energy calculations of complexes $(\boldsymbol{n})_1 \cdot M^+ \cdot (H_2O)_2$ ($\boldsymbol{n}$ = **1**–**5**; M^+ = Na^+ and K^+) were performed for polymers **1**–**5** in binding modes **A** (extended) and **B** (cyclic) (Figures 1b and S6–S9 and Table 1). The structures were optimized using the M06-2X/6-31G(d) level of theory, with energy calculated at the M06-2X/6-311+G(d,p) level. Our calculations indicate that, for Na^+, extended binding mode **A** is less stable than the cyclic

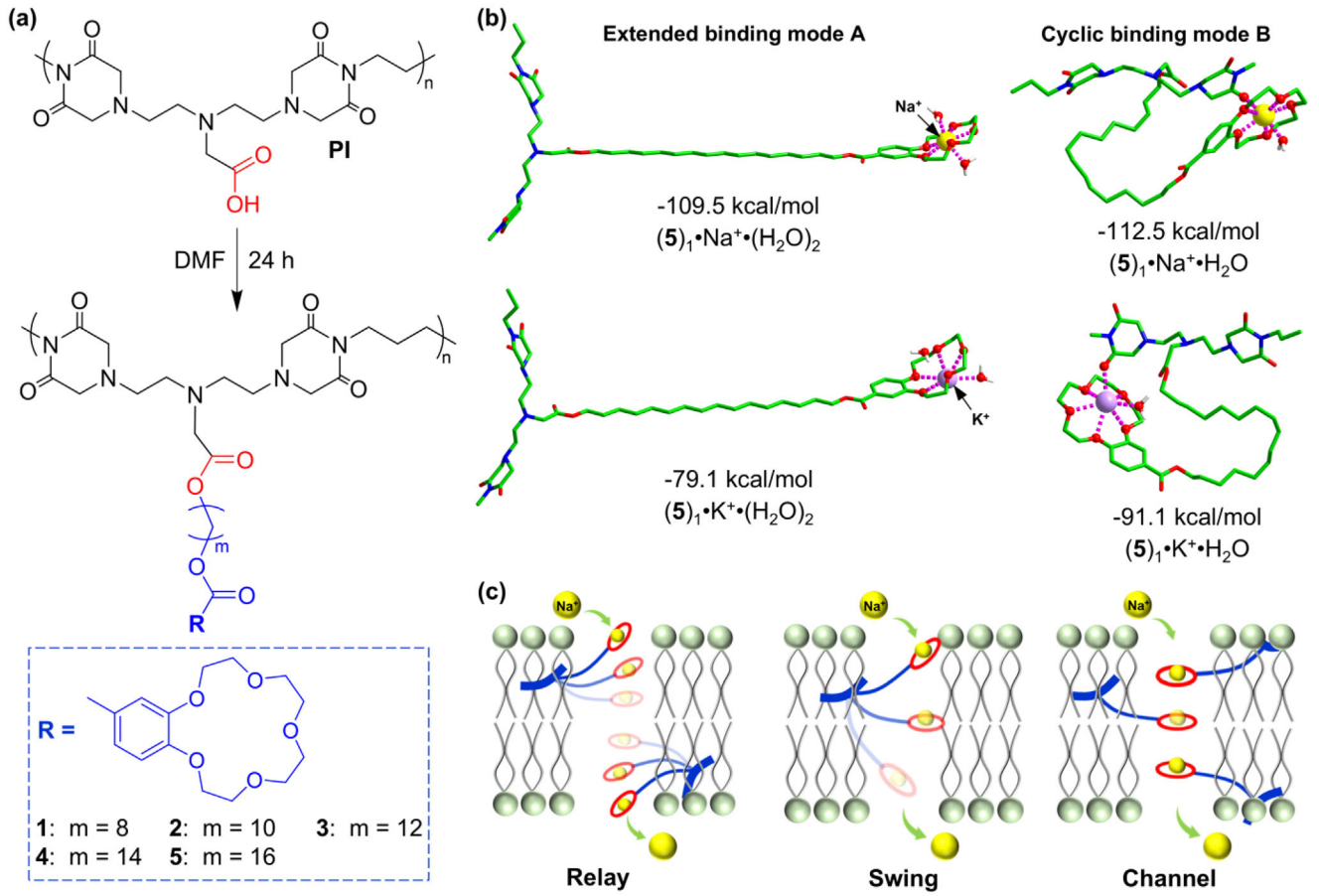

FIGURE 1 | Molecular design and schematic of a polyimide-based 15-crown-5-modified modular system as artificial Na^+-selective channels. (a) Synthesis of **PI**-based polymer channels **1**–**5**, bearing benzo-15-crown-5 structural units connected via alkyl chains of varying lengths. (b) DFT-optimized structures and binding energies for $(\mathbf{5})_1 \bullet Na^+ \bullet (H_2O)_2$ and $(\mathbf{5})_1 \bullet K^+ \bullet (H_2O)_2$ computed at the M06-2X/6-31G(d)//M06-2X/6-311+G(d,p) level of theory for extended binding mode **A** and cyclic binding mode **B**. (c) Schematic illustration of a channel molecule embedded in a lipid bilayer, depicting three possible ion transport mechanisms: molecular relay, molecular swing, and self-assembled channel formation. In the relay and channel mechanisms, the crown ether units involved in ion transport may originate from either a single polymer chain or from multiple polymer chains.

TABLE 1 | Calculated binding energies in kcal/mo[a] for polymers **1**–**5** in binding modes **A** and **B** (Figure 1b) for Na^+ and K^+ ions.

Ion	E[b]	1	2	3	4	5
Na^+	E_A	−108.4	−109.7	−108.7	−109.4	−109.5
	E_B	−117.9	−109.3	−110.9	−110.8	−112.5
	E_A_E_B	**9.5**	**0.4**	**2.2**	**1.4**	**3.0**
	E_{Na^+}_E_B	**16.2**	**7.6**	**9.2**	**9.1**	**10.8**
K^+	E_A	−78.5	−78.6	−80.9	−78.9	−91.1
	E_B	−93.8	−82.5	−91.9	−88.2	−79.1
	E_A_E_B	**15.3**	**3.9**	**11.0**	**9.3**	**12.0**
	E_{K^+}_E_B	**9.6**	**1.7**	**7.7**	**4.0**	**5.1**

[a]The energy calculations were carried out at the M06-2X/6-311+G (d,p) level.
[b]E_A and E_B represent the binding energies of modes **A** and **B**, respectively and the hydration energies of Na^+ (E_{Na^+}) and K^+ (E_{K^+}) are −101.7 and −84.2 kcal/mol. Bold values refer to the energy differences (E_A - E_B or E_M+ - E_B).

binding mode **B** by 9.5 kcal/mol for **1**, 2.2 kcal/mol for **3**, 1.4 kcal/mol for **4**, and 3.0 kcal/mol for **5**, except for **2**, with mode **A** slightly more stable than mode **B** by 0.4 kcal/mol. For K^+, mode **A** is less stable than mode **B** by 15.3 kcal/mol for **1**, 3.9 kcal/mol for **2**, 11.0 kcal/mol for **3**, 9.3 kcal/mol for **4**, and 12.0 kcal/mol for **5**. These comparative data suggest that the polymers preferentially adopt the thermodynamically favored mode **B** conformation for both Na^+ and K^+.

Interestingly, the energy difference between modes **A** and **B** for Na^+ binding across polymers **1**–**5** (0.4–9.5 kcal/mol) are notably smaller than that for K^+ binding (3.9–15.3 kcal/mol) (Table 1). This implies that Na^+ can switch more freely between the two binding modes, suggesting higher conformational flexibility during the ion capture and transport process.

Furthermore, after accounting for the hydration energy of Na^+ relative to the more stable mode **B**, the energies released for Na^+ binding by **1**–**5** range from 7.6 to 16.2 kcal/mol (Table 1). These values are consistently higher than those for K^+ (1.7–9.6 kcal/mol), indicating that binding of Na^+ is energetically more favorable than that of K^+. This stronger binding affinity for Na^+ may contribute to more efficient capture and ultimately enable highly efficient and selective transport of Na^+.

Prompted by the spectroscopic titration and computational findings, we quantified ion transport activities of crown ether-

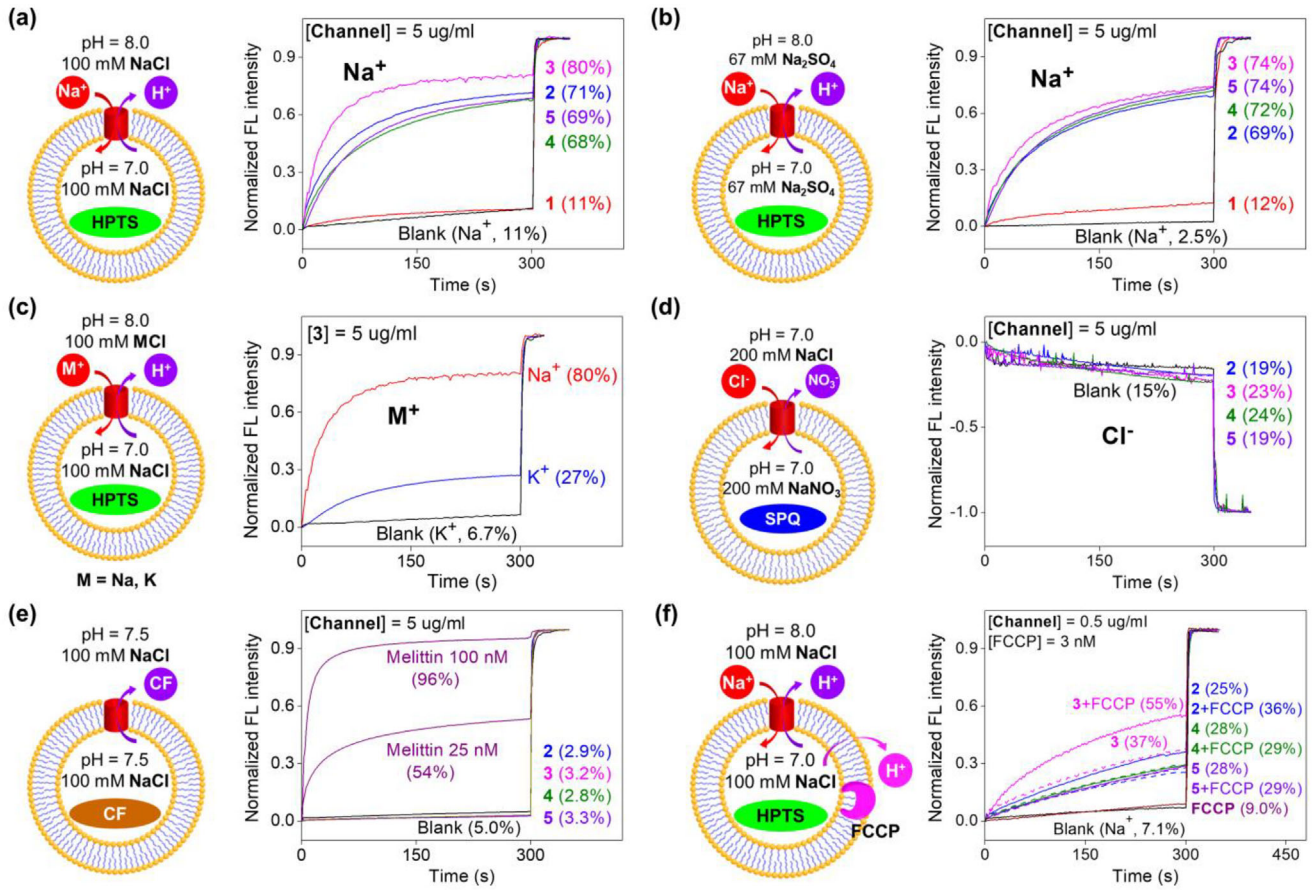

FIGURE 2 | (a–c) The DOPC-based pH-sensitive HPTS assay for comparing ion transport activities and selectivities of **1**–**5**, with extravesicular salts being NaCl or Na_2SO_4. (d) The chloride-sensitive SPQ assay for assessing the chloride transport activities of **2**–**5**. (e) CF dye leakage assay to confirm the membrane integrity in the presence of **2**–**5**. (f) The HPTS assay in the presence of proton carrier FCCP to compare the relative ion transport rate between H^+ and Na^+. DOPC = dioleoyl phosphatidylcholine, HPTS = 8-hydroxypyrene-1,3,6-trisulfonic acid trisodium salt, SPQ = (6-methoxy-N-(3-sulfopropyl))quinolinium, CF = 5(6)-carboxy fluorescein and FCCP = carbonyl cyanide 4-(trifluoromethoxy) phenylhydrazone.

functionalized **1**–**5** using a vesicle-based HPTS assay. This method employs pH-sensitive HPTS dye encapsulated within DOPC-based large unilamellar vesicles (LUVs), an imposed proton gradient (from pH 7.0 to 8.0) and extravesicular 100 mM KCl (Figure 2a). Using this method, **1** exhibits minimal Na^+ transport (15%, Figure 2a) at 5 μg/mL, while compounds **2**–**5** achieves 68%–80% transport, with **3** demonstrating the highest activity (Figure 2a). The data from the sulfate-loaded vesicular system further confirm efficient transport of Na^+ ions (Figure 2b). Using the same HPTS assay with extravesicular salts MCl or M_2SO_4 (M = Na and K, Figures 2c, S11, and S12), **2**–**5** exhibit remarkable Na^+ selectivity, with $EC_{50}(Na^+)$ values of 2.4, 1.2, 1.7 and 1.8 μg/mL, respectively (Figure S13), demonstrating highly active transport of Na^+ ions.

The anion transport activity of **2**–**5** was assessed using the SPQ fluorescence quenching assay, which utilizes a Cl^--sensitive fluorophore whose emission is selectively quenched by Cl^- ions. As illustrated in Figure 2d, **2**–**5** induce no significant change in SPQ fluorescence intensity at 5 μg/mL, confirming their inability to transport Cl^- ions.

Membrane integrity was evaluated using a CF dye leakage assay (Figures 2e and S14). At 5 μg/mL, **2**–**5** induce only 2.9-3.3% leakage, values that are far below the pore-forming control melittin, causing 54%and 96% leakage at 25 and 100 nM, respectively. These findings confirm the structural integrity of LUV membranes in the presence of **2**–**5** and therefore rule out membrane disruption or formation of large pores as mechanisms of ion transport by **2**–**5**.

To compare the relative rate between Na^+ and H^+, HPTS assays were conducted in the presence of a protonophore FCCP (Figure 2e). FCCP accelerates delayed H^+ counter-transport during Na^+ influx, producing fluorescence enhancement. After baseline correction, **2** and **3** show FCCP-dependent transport increases of 9% and 16%, respectively, confirming Na^+ flux as the dominant process. In contrast, **4** and **5** do not exhibit any enhancement, indicating that the carbon chain length has a significant influence on the transport of Na^+ ions. Single-channel electrophysiological studies using a planar lipid bilayer workstation were performed to quantify ion transport selectivity and elucidate mechanistic behavior of **2**–**5**.

Under symmetric ionic conditions (with 1 M NaCl present in both the *cis* and *trans* chambers; see Figure S15), channels **2**–**5** exhibit well-defined square-wave current traces, which unambiguously signify a channel-type ion transport mechanism (Figure 3a,c,e,g).

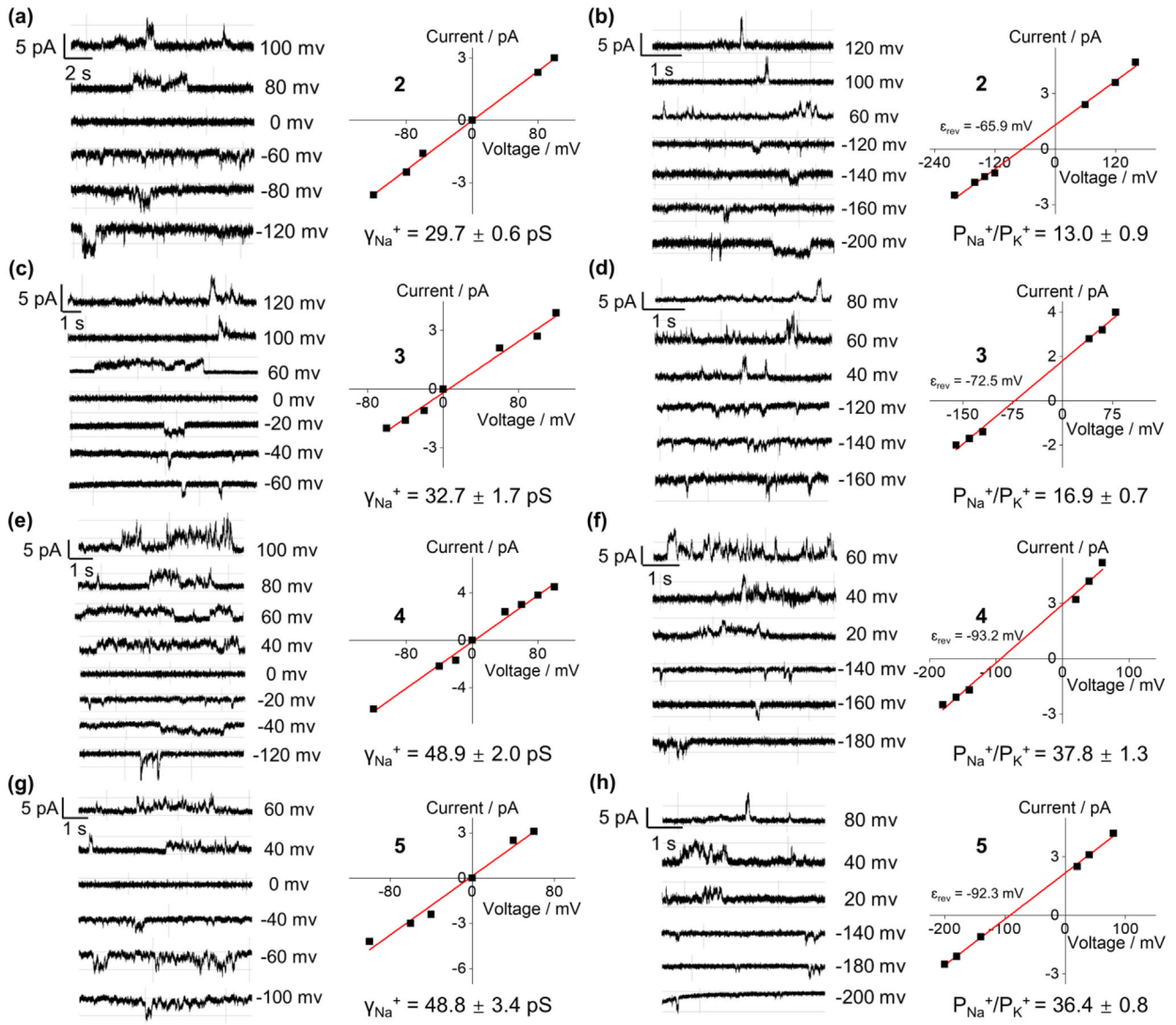

FIGURE 3 | Single channel current traces and current–voltage (I–V) curves recorded for **2**–**5**. (a), (c), (e), and (g) with *cis* chamber = *trans* chamber = 1 M NaCl; the potassium conduction rate (γ_{Na}^+) values were determined to be 29.7 ± 0.6 pS for **2** (a), 32.7 ± 1.7 pS for **3** (c), 48.9 ± 2.0 pS for **4** (e) and 48.8 ± 3.4 pS for **5** (g), respectively. (b), (d), (f), and (h) with *cis* chamber = 1 M NaCl and *trans* chamber = 1 M KCl, the P_{Na}^+/P_K^+ selectivity factors were determined to be 13.0 ± 0.9 for **2** (b), 16.9 ± 0.7 for **3** (d), 37.8 ± 1.3 for **4** (f), and 36.4 ± 0.8 for **5** (h), respectively. Here, γ_{Na}^+ values were obtained by fitting the I-V curves using a linear equation of y = a + b*x where slope b is γ in the unit of pS. P_{Na}^+/P_K^+ values were calculated using a simplified Goldman-Hodgkin-Katz equation $\varepsilon_{rev} = RT/F \times \ln(P_{Na}^+/P_K^+)$, where R = universal gas constant (8.314 J·K^{-1} mol^{-1}), T = 298 K, F = Faraday's constant (96 485 C·mol^{-1}), and P is the ion permeability. All single channel current traces were recorded in a diPhyPC-based bilayer membrane. diPhyPC = 1,2-diphytanoyl-sn-glycero-3-phosphocholine.

The measured unitary Na^+ conductance values (γ_{Na}^+) were 29.7 ± 0.6 pS for **2**, 32.7 ± 1.7 pS for **3**, 48.9 ± 2.0 pS for **4**, and 48.8 ± 3.4 pS for **5**. Based on the reported K^+ conductance of $\gamma_K^+ = 23.2 \pm 0.4$ pS for gramicidin A [31], **2**–**5** studied here demonstrate exceptional performance in Na^+ transport rate.

To evaluate Na^+/K^+ selectivity, experiments were conducted under asymmetric ionic conditions (1 M NaCl in the *cis* chamber and 1 M KCl in the *trans* chamber). Analysis of the current–voltage (I–V) relationships (Figure 3b,d,f,h) yields reversal potentials (ε_{rev}) of 65.9 mV for **2**, 72.5 mV for **3**, 93.2 mV for **4**, and 92.3 mV for **5**. These values correspond to Na^+/K^+ permeability ratios of 13.0 ± 0.9, 16.9 ± 0.7, 37.8 ± 1.3, and 36.4 ± 0.8, respectively. Particularly noteworthy is the performance of **4**, which exhibits the highest Na^+/K^+ selectivity of 37.8 and Na^+ ion conductance (48.9 ± 2.0 pS) reported to date. These results demonstrate that this design strategy has successfully alleviated the long-standing trade-off in artificial Na^+ channel, i.e., the difficulty in simultaneously achieving both high ion transport rates and selectivity.

Interestingly, the side-chain length appears to exert a significant influence on both the ion transport activity and selectivity. Specifically, channels **2**–**5** exhibit transport efficiency and selectivity

that increase in the order **2** < **3** < **4** ≈ **5** with increasing side-chain length. In their fully extended states, the side-chain lengths of **2**–**5** are 1.88, 2.12, 2.38, and 2.63 nm, respectively, matching progressively well with the typical hydrophobic membrane thickness of 3 nm. Among the three proposed ion transport mechanisms (swinging, relay, and channel-like mechanisms; Figure 1c) and further given that longer alkyl chains may better span the membrane hydrophobic region, these findings possibly may suggest that swinging and relay mechanisms are the two dominant mechanisms, accounting for the higher transport efficiencies observed for channels **4** and **5** compared with **2** and **3**. Nevertheless, it is difficult to establish a correlation between the selectivity properties and the side-chain length.

In summary, by employing a modular design that integrates a flexible polyimide backbone, tunable alkyl spacers, and 15-crown-5 ionophores, we have designed and synthesized a series of crown-ether-functionalized polyimide polymers. These structurally well-defined systems (**2**–**5**) enable highly efficient and selective transmembrane Na^+ transport, exhibiting a remarkable Na^+ conductance of 48.9 pS and a record-high Na^+/K^+ selectivity of up to 37.8. This strategy establishes a new paradigm for the rational design of high-performance Na^+-selective artificial channels and opens promising avenues for the development of therapeutics targeting disorders associated with dysregulated Na^+ transport.

Acknowledgments

We greatly appreciate the support of this work by the National Natural Science Foundation of China (22271049 and 22371048), the "Chu ying Program" for the Top Young Talents of Fujian Province, the Postdoctoral Fellowship Program of CPSF under Grant Number GZC20230455, the Natural Science Foundation of Fujian Province (2023J01054) and a start-up grant from Fuzhou University.

Conflicts of Interest

The authors declare no conflicts of interest.

Data Availability Statement

The data that support the findings of this study are available from the corresponding author upon reasonable request.

References

1. J. Letarte and A. E. Renold, "Glucose Metabolism in Fat Cells Stimulated by Insulin and Dependent on Sodium," *Nature* 215 (1967): 961–962, https://doi.org/10.1038/215961a0.

2. W. A. Catterall, "From Ionic Currents to Molecular Mechanisms," *Neuron* 26 (2000): 13–25, https://doi.org/10.1016/S0896-6273(00)81133-2.

3. Y. Yin, Y. Song, Y. Jia, J. Xia, R. Bai, and X. Kong, "Sodium Dynamics in the Cellular Environment," *Journal of the American Chemical Society* 145 (2023): 10522–10532, https://doi.org/10.1021/jacs.2c13271.

4. L. G. Palmer, "Epithelial Na Channels: Function and Diversity," *Annual Review of Physiology* 54 (1992): 51–66, https://doi.org/10.1146/annurev.ph.54.030192.000411.

5. D. G. Warnock, K. Kusche-Vihrog, A. Tarjus, et al., "Blood Pressure and Amiloride-Sensitive Sodium Channels in Vascular and Renal Cells," *Nature Reviews Nephrology* 10 (2014): 146–157, https://doi.org/10.1038/nrneph.2013.275.

6. J. J. Kasianowicz, "Introduction to Ion Channels and Disease," *Chemical Reviews* 112 (2012): 6215–6217, https://doi.org/10.1021/cr300444k.

7. W. Hang, M. Liu, S. F. Yan, and N. Yan, *Protein & Cell* 8 (2017): 401–438.

8. E. Gouaux and R. MacKinnon, "Principles of Selective Ion Transport in Channels and Pumps," *Science* 310 (2005): 1461–1465, https://doi.org/10.1126/science.1113666.

9. T. M. Fyles, "Synthetic Ion Channels in Bilayer Membranes," *Chemical Society Reviews* 36 (2007): 335–347, https://doi.org/10.1039/B603256G.

10. H. Zhang, X. Li, J. Hou, L. Jiang, and H. Wang, "Angstrom-Scale Ion Channels Towards Single-Ion Selectivity," *Chemical Society Reviews* 51 (2022): 2224–2254, https://doi.org/10.1039/D1CS00582K.

11. J. T. Davis, O. Okunola, and R. Quesada, "Recent Advances in the Transmembrane Transport of Anions," *Chemical Society Reviews* 39 (2010): 3843, https://doi.org/10.1039/b926164h.

12. F. Otis, M. Auger, and N. Voyer, "Exploiting Peptide Nanostructures To Construct Functional Artificial Ion Channels," *Accounts of Chemical Research* 46 (2013): 2934–2943, https://doi.org/10.1021/ar400044k.

13. Y.-M. Legrand and M. Barboiu, "Self-Assembled Supramolecular Channels: Toward Biomimetic Materials for Directional Translocation," *Chemical Record* 13 (2013): 524–538, https://doi.org/10.1002/tcr.201300011.

14. J. Montenegro, M. R. Ghadiri, and J. R. Granja, "Ion Channel Models Based on Self-Assembling Cyclic Peptide Nanotubes," *Accounts of Chemical Research* 46 (2013): 2955–2965, https://doi.org/10.1021/ar400061d.

15. N. Busschaert, C. Caltagirone, W. Van Rossom, and P. A. Gale, "Applications of Supramolecular Anion Recognition," *Chemical Reviews* 115 (2015): 8038–8155, https://doi.org/10.1021/acs.chemrev.5b00099.

16. M. Barboiu, "Encapsulation versus Self-Aggregation Toward Highly Selective Artificial K + Channels," *Accounts of Chemical Research* 51 (2018): 2711–2718, https://doi.org/10.1021/acs.accounts.8b00311.

17. M. J. Langton, "Engineering of Stimuli-Responsive Lipid-Bilayer Membranes Using Supramolecular Systems," *Nature Reviews Chemistry* 5 (2021): 46–61.

18. J. Yang, G. Yu, J. L. Sessler, I. Shin, and P. A. Gale, "Artificial Transmembrane Ion Transporters as Potential Therapeutics," *Chemistry* 7 (2021): 3256–3291, https://doi.org/10.1016/j.chempr.2021.10.028.

19. S.-P. Zheng, L.-B. Huang, Z. Sun, and M. Barboiu, "Self-Assembled Artificial Ion-Channels Toward Natural Selection of Functions," *Angewandte Chemie International Edition* 60 (2021): 566–597, https://doi.org/10.1002/anie.201915287.

20. J. Shen, C. L. Ren, and H. Q. Zeng, "Membrane-Active Molecular Machines," *Accounts of Chemical Research* 55 (2022): 1148–1159, https://doi.org/10.1021/acs.accounts.1c00804.

21. J. de Jong, J. E. Bos, and S. J. Wezenberg, "Stimulus-Controlled Anion Binding and Transport by Synthetic Receptors," *Chemical Reviews* 123 (2023): 8530–8574, https://doi.org/10.1021/acs.chemrev.3c00039.

22. A. Singh, A. Torres-Huerta, F. Meyer, and H. Valkenier, "Anion Transporters Based on Halogen, Chalcogen, and Pnictogen Bonds: Towards Biological Applications," *Chemical Science* 15 (2024): 15006–15022, https://doi.org/10.1039/D4SC04644G.

23. X. Y. Yuan, J. Shen, and H. Q. Zeng, "Artificial Transmembrane Potassium Transporters: Designs, Functions, Mechanisms and Applications," *Chemical Communications* 60 (2024): 482–500, https://doi.org/10.1039/D3CC04488B.

24. D. Y. Zhang, W. J. Chang, J. Shen, and H. Q. Zeng, "Aromatic Foldamer-Derived Transmembrane Transporters," *Chemical Communications* 60 (2024): 13468–13491, https://doi.org/10.1039/D4CC04388J.

25. U. M. C. Rathnaweera, S. M. Chowdhury, R. Salam, and N. Busschaert, "Medical and Nonmedical Applications of Synthetic Transmembrane Anion Transporters," *Chemical Reviews* 125 (2025): 8370–8425, https://doi.org/10.1021/acs.chemrev.5c00129.

26. T. Yan and J. Liu, "Transmembrane Ion Channels: From Natural to Artificial Systems," *Angewandte Chemie International Edition* 64 (2025): e16200, https://doi.org/10.1002/anie.202416200.

27. S. Liu, H. Liu, J. Jiang, G. Liu, and J. Liu, "Molecular Machines for Transmembrane Ion Transport," *Chemical Communications* 61 (2025): 14598–14610, https://doi.org/10.1039/D5CC03010B.

28. M. R. Ghadiri, J. R. Granja, and L. K. Buehler, "Artificial Transmembrane Ion Channels From Self-assembling Peptide Nanotubes," *Nature* 369 (1994): 301–304, https://doi.org/10.1038/369301a0.

29. N. Busschaert and P. A. Gale, "Small-Molecule Lipid-Bilayer Anion Transporters for Biological Applications," *Angewandte Chemie International Edition* 52 (2013): 1374–1382, https://doi.org/10.1002/anie.201207535.

30. G. Su, M. Zhang, W. Si, Z.-T. Li, and J.-L. Hou, "Directional Potassium Transport Through a Unimolecular Peptide Channel," *Angewandte Chemie International Edition* 55 (2016): 14678–14682, https://doi.org/10.1002/anie.201608428.

31. C. L. Ren, J. Shen, and H. Q. Zeng, "Combinatorial Evolution of Fast-Conducting Highly Selective K + -Channels via Modularly Tunable Directional Assembly of Crown Ethers," *Journal of the American Chemical Society* 139 (2017): 12338–12341, https://doi.org/10.1021/jacs.7b04335.

32. S. Chen, Y. Wang, T. Nie, et al., "An Artificial Molecular Shuttle Operates in Lipid Bilayers for Ion Transport," *Journal of the American Chemical Society* 140 (2018): 17992–17998, https://doi.org/10.1021/jacs.8b09580.

33. L. Z. Zeng, H. Zhang, T. Wang, and T. Li, "Enhancing K^+ Transport Activity and Selectivity of Synthetic K^+ Channels via Electron-Donating Effects," *Chemical Communications* 56 (2020): 1211–1214, https://doi.org/10.1039/C9CC08396K.

34. W.-L. Huang, X.-D. Wang, Y.-F. Ao, Q.-Q. Wang, and D.-X. Wang, "Artificial Chloride-Selective Channel: Shape and Function Mimic of the ClC Channel Selective Pore," *Journal of the American Chemical Society* 142 (2020): 13273–13277, https://doi.org/10.1021/jacs.0c02881.

35. D. Qiao, H. Joshi, H. Zhu, et al., "Synthetic Macrocycle Nanopore for Potassium-Selective Transmembrane Transport," *Journal of the American Chemical Society* 143 (2021): 15975–15983, https://doi.org/10.1021/jacs.1c04910.

36. Z.-J. Yan, Y.-W. Li, M. Yang, et al., "Voltage-Driven Flipping of Zwitterionic Artificial Channels in Lipid Bilayers to Rectify Ion Transport," *Journal of the American Chemical Society* 143 (2021): 11332–11336, https://doi.org/10.1021/jacs.1c06000.

37. S. Qi, C. Zhang, H. Yu, et al., "Foldamer-Based Potassium Channels With High Ion Selectivity and Transport Activity," *Journal of the American Chemical Society* 143 (2021): 3284–3288, https://doi.org/10.1021/jacs.0c12128.

38. H. Yang, J. Yi, S. Pang, et al., "A Light-Driven Molecular Machine Controls K^+ Channel Transport and Induces Cancer Cell Apoptosis," *Angewandte Chemie International Edition* 61 (2022): e202204605, https://doi.org/10.1002/anie.202204605.

39. T. G. Johnson, A. Sadeghi-Kelishadi, and M. J. Langton, "A Photo-Responsive Transmembrane Anion Transporter Relay," *Journal of the American Chemical Society* 144 (2022): 10455–10461, https://doi.org/10.1021/jacs.2c02612.

40. T. G. Johnson and M. J. Langton, "Molecular Machines for the Control of Transmembrane Transport," *Journal of the American Chemical Society* 145 (2023): 27167–27184, https://doi.org/10.1021/jacs.3c08877.

41. L. Zhang, C. Zhang, X. Dong, and Z. Dong, "Highly Selective Transmembrane Transport of Exogenous Lithium Ions Through Rationally Designed Supramolecular Channels," *Angewandte Chemie International Edition* 62 (2023): e14194.

42. H. W. Ma, R. J. Ye, L. Jin, et al., "Highly Active Artificial Potassium Channels Having Record-High K^+/Na^+ Selectivity of 20.1," *Chinese Chemical Letters* 34 (2023): 108355, https://doi.org/10.1016/j.cclet.2023.108355.

43. A. Mondal, S. N. Save, S. Sarkar, et al., "A Benzohydrazide-Based Artificial Ion Channel That Modulates Chloride Ion Concentration in Cancer Cells and Induces Apoptosis by Disruption of Autophagy," *Journal of the American Chemical Society* 145 (2023): 9737–9745, https://doi.org/10.1021/jacs.3c01451.

44. R. Cao, R. B. Rossdeutcher, Y. Zhong, et al., "Aromatic Pentaamide Macrocycles Bind Anions With High Affinity for Transport Across Biomembranes," *Nature Chemistry* 15 (2023): 1559–1568, https://doi.org/10.1038/s41557-023-01315-w.

45. S. Deng, Z. Li, L. Yuan, J. Shen, and H. Q. Zeng, "Light-Powered Propeller-Like Transporter for Boosted Transmembrane Ion Transport," *Nano Letters* 24 (2024): 10750–10758, https://doi.org/10.1021/acs.nanolett.4c01884.

46. Q. Zhang, Q. Liang, G. Wang, et al., "Highly Selective Artificial K+ Transporters Reverse Liver Fibrosis In Vivo," *JACS Au* 4 (2024): 3869–3883.

47. Y. Wu, Q. Xu, Y. Chen, et al., "Mechanosensitive and pH-Gated Butterfly-Shaped Artificial Ion Channel for High-Selective K+ Transport and Cancer Cell Apoptosis," *Advanced Materials* 37 (2025): 2416852, https://doi.org/10.1002/adma.202416852.

48. A. Roy, J. Shen, H. Joshi, et al., "Foldamer-Based Ultrapermeable and Highly Selective Artificial Water Channels That Exclude Protons," *Nature Nanotechnology* 16 (2021): 911–917, https://doi.org/10.1038/s41565-021-00915-2.

49. J. Shen, Y. Zhang, Y. Jin, et al., "Butterfly-Shaped Folding Synthons for Designing Superselective and Ultrapermeable Artificial Water Channels," *Angewandte Chemie International Edition* 64 (2025): e06341, https://doi.org/10.1002/anie.202506341.

50. J. Shen, R. Ye, Z. Liu, and H. Q. Zeng, "Hybrid Pyridine–Pyridone Foldamer Channels as M2-Like Artificial Proton Channels," *Angewandte Chemie International Edition* 61 (2022): e202200259, https://doi.org/10.1002/anie.202200259.

51. F. Gou, Y. Yao, Q. Wang, et al., "Flexible Crown-Ether Polyimides Break the K^+/Na^+ Selectivity Barrier in Artificial K^+ Channels," *Angewandte Chemie International Edition* 65 (2026): e20146, https://doi.org/10.1002/anie.202520146.

52. J. Shen, D. R., Z. Li, H. Oh, et al., "Sulfur-Containing Foldamer-Based Artificial Lithium Channels," *Angewandte Chemie International Edition* 62 (2023): e202305623, https://doi.org/10.1002/anie.202305623.

53. F. Gou, Q. Wang, Z. Yang, W. Chang, J. Shen, and H. Q. Zeng, "Artificial Lithium Channels Built From Polymers With Intrinsic Microporosity," *Angewandte Chemie International Edition* 64 (2025): e18304, https://doi.org/10.1002/anie.202418304.

54. F. Gou, Z. Yang, Q. Wang, W. Chang, J. Shen, and H. Q. Zeng, "Chirality-Induced Split Personality in Polymer With Intrinsic Microporosity-Based Artificial Ion Channels," *Angewandte Chemie International Edition* 64 (2025): e16573, https://doi.org/10.1002/anie.202516573.

55. O. Murillo, S. Watanabe, and G. W. G. A. Nakano, "Synthetic Models for Transmembrane Channels: Structural Variations That Alter Cation Flux," *Journal of the American Chemical Society* 117 (1995): 7665–7679, https://doi.org/10.1021/ja00134a011.

56. F. Otis, C. Racine-Berthiaume, and N. Voyer, "How Far Can a Sodium Ion Travel Within a Lipid Bilayer?," *Journal of the American Chemical Society* 133 (2011): 6481–6483, https://doi.org/10.1021/ja110336s.

57. Y. H. Li, S. Zheng, Y.-M. Legrand, A. Gilles, A. Van der Lee, and M. Barboiu, "Structure-Driven Selection of Adaptive Transmembrane Na^+ Carriers or K^+ Channels," *Angewandte Chemie International Edition* 57 (2018): 10520–10524, https://doi.org/10.1002/anie.201802570.

58. S. Qi, J. Tian, J. Zhang, et al., "Unimolecular Transmembrane Na^+ Channels Constructed by Pore-Forming Helical Polymers With a 2.3 Å

Aperture," *CCS Chemistry* 4 (2022): 1850–1857, https://doi.org/10.31635/ccschem.021.202101144.

59. L. Zhang, J. Tian, Z. Lin, and Z. Dong, "Efficient Sodium Transmembrane Permeation Through Helically Folded Nanopores With Natural Channel-Like Ion Selectivity," *Journal of the American Chemical Society* 146 (2024): 8500–8507, https://doi.org/10.1021/jacs.3c14736.

60. T. Jiang, A. Hall, M. Eres, Z. Hemmatian, et al., "Single-chain Heteropolymers Transport Protons Selectively and Rapidly," *Nature* 577 (2020): 216–220, https://doi.org/10.1038/s41586-019-1881-0.

61. J. Shen, J. Fan, R. Ye, N. Li, Y. Mu, and H. Q. Zeng, "Polypyridine-Based Helical Amide Foldamer Channels: Rapid Transport of Water and Protons With High Ion Rejection," *Angewandte Chemie International Edition* 59 (2020): 13328–13334, https://doi.org/10.1002/anie.202003512.

62. F. Chen, J. Shen, N. Li, et al., "Pyridine/Oxadiazole-Based Helical Foldamer Ion Channels With Exceptionally High K^+ /Na^+ Selectivity," *Angewandte Chemie International Edition* 59 (2020): 1440–1444, https://doi.org/10.1002/anie.201906341.

63. T. Yan, S. Liu, C. Li, et al., "Flexible Single-Chain-Heteropolymer-Derived Transmembrane Ion Channels With High K^+ Selectivity and Tunable pH-Gated Characteristics," *Angewandte Chemie International Edition* 61 (2022): e10214, https://doi.org/10.1002/anie.202210214.

64. C. Li, Y. Wu, Y. Zhu, et al., "Molecular Motor-Driven Light-Controlled Logic-Gated K^+ Channel for Cancer Cell Apoptosis," *Advanced Materials* 36 (2024): 2312352, https://doi.org/10.1002/adma.202312352.

65. Y. Lin, B. Wu, Y. Zeng, et al., "Artificial Channels Based on Bottlebrush Polymers: Enhanced Ion Transport through Polymer Topology Control," *Angewandte Chemie International Edition* 63 (2024): e202408558, https://doi.org/10.1002/anie.202408558.

66. C. Li, Y. Wu, S. Bao, et al., "Photo-Switchable Supramolecular Interactions Regulate K^+ Transmembrane Transport and Cancer Cell Apoptosis," *Journal of the American Chemical Society* 147 (2025): 14139–14153, https://doi.org/10.1021/jacs.4c14583.

67. D.-J. Liaw, K.-L. Wang, Y.-C. Huang, K.-R. Lee, J.-Y. Lai, and C.-S. Ha, "Advanced Polyimide Materials: Syntheses, Physical Properties and Applications," *Progress in Polymer Science* 37 (2012): 907–974, https://doi.org/10.1016/j.progpolymsci.2012.02.005.

68. I. Gouzman, E. Grossman, R. Verker, N. Atar, A. Bolker, and N. Eliaz, "Advances in Polyimide-Based Materials for Space Applications," *Advanced Materials* 31 (2019): 1807738, https://doi.org/10.1002/adma.201807738.

69. Y. Zhuang, J. G. Seong, and Y. M. Lee, "Polyimides Containing Aliphatic/Alicyclic Segments in the Main Chains," *Progress in Polymer Science* 92 (2019): 35–88, https://doi.org/10.1016/j.progpolymsci.2019.01.004.

70. T. W. Allen, O. S. Andersen, and B. Roux, "On the Importance of Atomic Fluctuations, Protein Flexibility, and Solvent in Ion Permeation," *Journal of General Physiology* 124 (2004): 679–690, https://doi.org/10.1085/jgp.200409111.

71. T. Baştuğ, A. Gray-Weale, S. M. Patra, and S. Kuyucak, *Biophysical Journal* 90 (2006): 2285–2296.

72. C. Boiteux, I. Vorobyov, and T. W. Allen, "Ion Conduction and Conformational Flexibility of a Bacterial Voltage-Gated Sodium Channel," *PNAS* 111 (2014): 3454–3459, https://doi.org/10.1073/pnas.1320907111.

73. B. Roux, "Ion Channels and Ion Selectivity," *Essays in Biochem* 61 (2017): 201–209.

74. W. Coyote-Maestas, D. Nedrud, A. Suma, et al., "Probing Ion Channel Functional Architecture and Domain Recombination Compatibility By Massively Parallel Domain Insertion Profiling," *Nature Communications* 12 (2021): 7114.

75. B. A. McNally, E. J. O'Neil, A. Nguyen, and B. D. Smith, "Membrane Transporters for Anions That Use a Relay Mechanism," *Journal of the American Chemical Society* 130 (2008): 17274–17275, https://doi.org/10.1021/ja8082363.

76. R. Ye, C. Ren, J. Shen, et al., "Molecular Ion Fishers as Highly Active and Exceptionally Selective K^+ Transporters," *Journal of the American Chemical Society* 141 (2019): 9788–9792, https://doi.org/10.1021/jacs.9b04096.

77. C. Ren, F. Chen, R. Ye, et al., "Molecular Swings as Highly Active Ion Transporters," *Angewandte Chemie International Edition* 58 (2019): 8034–8038, https://doi.org/10.1002/anie.201901833.

78. H. Zhang, R. Ye, Y. Mu, Y. Li, and H. Q. Zeng, "Small Molecule-Based Highly Active and Selective K^+ Transporters With Potent Anticancer Activities," *Nano Letters* 21 (2021): 1384–1391, https://doi.org/10.1021/acs.nanolett.0c04134.

Supporting Information

Additional supporting information can be found online in the Supporting Information section.

Supporting File: anie72298-sup-0001-SuppMat.Pdf.